2017

Effects of Recycled HDPE and Nanoclay on Stress Cracking of HDPE by Correlating J_c with Slow Crack Growth

Sukjoon Na
Drexel University

Long Nguyen
Drexel University

Sabrina Spatari
Drexel University

Yick G. Hsuan
Drexel University, ghsuan@coe.drexel.edu

Effects of Recycled HDPE and Nanoclay on Stress Cracking of HDPE by Correlating J_c with Slow Crack Growth

Sukjoon Na, Long Nguyen, Sabrina Spatari, Yick G. Hsuan
Department of Civil, Architectural and Environmental Engineering, Drexel University, Philadelphia, PA

The effects of recycled high density polyethylene (HDPE) and nanoclay on the stress crack resistance (SCR) of pristine HDPE were evaluated using the Notched Constant Ligament Stress (NCLS) test. The test data were analyzed by both linear elastic fracture mechanics (LEFM) and elastic plastic fracture mechanics (EPFM). The LEFM approach uses the stress intensity factor *K* to define the two failure mechanisms: creep and slow crack growth (SCG). In contrast, using the *J*-integral in EPFM, which emphasizes the nonlinear elastic-plastic strain field at the crack-tip, revealed a short-term failure stage prior to the creep failure. In this article, a power law correlation between the fracture toughness J_c and SCG was found under a plane-strain condition. Increasing recycled HDPE content lowered the SCG resistance of pristine HDPE by decreasing J_c. Adding nanoclay up to 6 wt% also decreased J_c while simultaneously, lowering the stress relaxation of nanocomposites, leading to longer SCG failure times at low *J* values.
POLYM. ENG. SCI., 00:000–000, 2017. Published [2017].

INTRODUCTION

In the past few decades, high density polyethylene (HDPE) has been increasingly used in civil engineering and environmental engineering infrastructure, particularly for drainage pipe systems. With good mechanical properties, corrosion resistance, ease of manufacturing, and favorable economics, HDPE has continuously replaced conventional pipe materials such as steel, concrete and other plastics. However, current HDPE pipe used in infrastructure is made from pristine resins which rely on petroleum and natural gas feedstock supply, and thus deplete finite resources whose extraction and processing consumes substantial energy and releases greenhouse gases (GHG) to the atmosphere [1]. On the other hand, an increase in the use of HDPE in consumer products as well as in engineering applications has prompted concern about accumulating plastic waste due to its permanence in the environment. To improve the environmental sustainability of HDPE pipe and propose a solution to these concerns, the use of recycled polyethylene for pipe materials was considered in this study. Using recycled HDPE to replace a portion of pristine HDPE resin certainly provides benefits in lowering the overall cost of raw materials and reducing environmental impacts [1].

Challenges still remain, however, with respect to the stress crack resistance (SCR) of HDPE pipe over its design life when recycled HDPE is blended with the pristine resin. Increasing recycled content in a pristine/recycled HDPE blend is likely to reduce SCR and increase the risk of cracking within the service life. For example, Stefanovski *et al*. [2] and Hsuan [3] reported that SCR of recycled polyethylene is lower than that of the pristine PE resin. To improve SCR of recycled HDPE blends, this study focused on nanoclay-reinforced composites. Polymer/clay nanocomposites (PCNs) have received considerable attention due to their improved material properties. Incorporating a small amount of nanoclay into a polymer matrix can significantly enhance the tensile strength, surface scratch resistance, and flammability resistance while decreasing gas permeability [4–6]. However, the effect of nanoclay on SCR of the pristine and recycled HDPE blends has not been thoroughly studied. By understanding this effect, a plastic pipe made from pristine and recycled HDPE blends could be engineered with the inclusion of a small concentration of nanoclay in order to achieve comparable performance to the pristine HDPE.

SCR of HDPE has been extensively studied and the majority of the experimental tests are performed at elevated temperatures to accelerate crack propagation. Methods to extrapolate data from elevated temperature tests to a lower ambient temperature include the rate process method (RPM) and Popelar shift method (PSM). RPM is evolved from the Arrhenius principle of time-temperature superposition [7]. On the other hand, the Popelar's shift method utilizes two empirical equations for shifting individual applied stress and failure time test data from an elevated temperature to a lower temperature [8, 9]. Recently, McCarthy *et al*. [10] correlated the uniaxial tensile strain-hardening property of PE with SCR based on the hypothesis that the intrinsic strain hardening behavior is similar to the fibril failure inside the craze, and the test procedure was standardized as ISO 18488 [11].

From the fracture mechanics point of view, the fracture failure of a material is defined by the plane-strain fracture toughness (K_c or J_c), and is determined using a short-term time-independent tests. On the other hand, stress cracking caused by a slow crack growth (SCG) mechanism is evaluated using a time-dependent tests while the fracture toughness is ignored. Several studies [12–15] presented correlations between the time-independent fracture toughness and time-dependent SCG, but these correlations were based on linear elastic fracture mechanics (LEFM) and may not be appropriate to apply to nonlinear elastic-plastic materials. This article discusses a new approach to correlate SCG to the fracture toughness based on elastic-plastic fracture mechanics (EPFM). The SCG behavior was evaluated using the notched constant ligament stress (NCLS) test, while the fracture toughness was determined in our previous papers using the essential work of fracture (EWF) concept [16, 17]. The correlation concept was studied on recycled HDPE materials [18]. In this paper, we further elaborate on the correlation approach and present the effect of recycled HDPE and

Correspondence to: Y. G. Hsuan; e-mail: ghsuan@coe.drexel.edu
The work presented here has been supported by National Science Foundation (NSF CMMI – 1030783).
DOI 10.1002/pen.24691
Published online in Wiley Online Library (wileyonlinelibrary.com).

nanoclay on short-term and long-term stress cracking behavior of HDPE.

EXPERIMENTAL

Materials

The pristine HDPE resin (ExxonMobil™ HDPE HD 7800P) with density of 0.954 g/cm^3 and melt index (MI) of 0.230 g/10 min was provided by ExxonMobil™. The recycled HDPE pellets with density 0.961 g/cm^3 and MI of 0.642 g/10 min, which were collected and reprocessed from milk jugs and water bottles, were supplied by Envision Plastics. Organo-modified montmorillonite (Nanomer® 1.44P) containing a surface modifier (dehydrogenated tallow dimethyl ammonium) was provided by Nanocor in the form of a master batch consisting of 50% nanoclay and 50% PE. Recycle-blends were prepared by mixing recycled HDPE pellets with pristine HDPE resin with weight fractions of 25, 50, and 75%. PCNs were made from blending the prepared recycle-blends with the appropriate amount of nanoclay master batch to achieve the target concentration of 2, 4, and 6% by weight. The recycle-blends and PCNs were then produced in the form of pellets using a laboratorial twin-screw extruder. Subsequently, the pellets were compression molded into plaques with dimensions of 170 mm × 170 mm and with thickness of 2-mm according to ASTM D 4703-Procedure A [19]. In this study, test materials were coded on the basis of the material composition. For example, P25R75/2% referred to the blend consisting of 25% pristine HDPE and 75% recycled HDPE with 2% nanoclay by weight.

Crystallinity Measurement

The percent crystallinity of test materials was measured using a TA instrument Q20 differential scanning calorimeter (DSC). Three replicates weighting between 3.5 and 4 mg were taken from each material. The specimens were then heated from room temperature to 200°C at a rate of 10°C/min in a nitrogen atmosphere according to ASTM D 3418 [20]. The crystallinity was calculated by integrating the melting curve between 60°C and 150°C.

Uniaxial Tensile Test

The uniaxial tensile testing was carried out using a universal testing machine (Instron 5567) according to ASTM D638 [21] at a strain rate of 5 mm/min. The type IV dumbbell-shaped specimens were cut from the 2-mm thick compression molded plaque. The tensile strain was measured using an extensometer with a gauge length of 25 mm. The secant modulus at 1.5% of strain and corresponding stress were used to represent the elastic modulus and yield stress based on the elastic-plastic model [16, 17].

Stress Crack Resistance (SCR) Test

The SCR property was evaluated using the Notched Constant Ligament Stress (NCLS) test according to ASTM F 2136 [22]. The dumbbell-shape specimens with dimensions of 3.175 mm wide (W) × 2 mm thick (t) × 63.5 mm long (L), were die out from a 2-mm thick compression molded plaque. Each test specimen was notched to a depth of 20% of the specimen thickness (i.e., 0.4 mm) using a razor blade at a rate of 0.1 in/min. The notched specimens were then fixed onto the test modules which were then immersed into a bath with distilled water at a temperature of either 30°C or 70°C. At a temperature of 30°C, applied stresses from 15 to 22 MPa were tested to achieve ductile failures within measurable times. For tests carried out at 70°C, stresses from 1.4 to 9 MPa were applied to capture the brittle failures. The failure time was recorded to the accuracy of ±1.0 seconds for ductile failures and ±0.1 hours for brittle failures.

The effect of recycled HDPE on the SCR of pristine HDPE resin was assessed by testing samples of P75R25, P50R50 and P25R75, whereas the influence of nanoclay on the recycled blended HDPE materials was investigated by testing P25R75 with 2, 4, and 6 wt% of nanoclay.

TABLE 1. Crystallinity and tensile properties of tested materials.

Blends	Clay content (%)	Crystallinity (%)	Elastic Modulus (MPa)	Yield Stress (MPa)
P75R25	0	68.3 ± 1.1	895.7 ± 25.8	13.4 ± 0.4
	2	70.2 ± 0.7	1,002.4 ± 6.7	15.0 ± 0.1
	4	67.1 ± 0.2	1,015.9 ± 21.6	15.2 ± 0.3
	6	64.3 ± 1.1	1,021.0 ± 3.2	15.6 ± 0.2
P50R50	0	68.8 ± 0.3	909.0 ± 12.4	13.6 ± 0.2
	2	67.1 ± 0.4	1,048.9 ± 21.4	15.7 ± 0.3
	4	67.9 ± 1.1	1,069.3 ± 7.7	16.0 ± 0.1
	6	67.9 ± 0.7	1,091.3 ± 15.6	16.4 ± 0.2
P25R75	0	71.7 ± 1.1	930.2 ± 10.6	14.0 ± 0.2
	2	68.7 ± 1.2	1,081.6 ± 13.8	16.2 ± 0.2
	4	65.4 ± 1.5	1,077.4 ± 4.6	16.2 ± 0.1
	6	64.9 ± 0.9	1,061.6 ± 4.6	15.9 ± 0.1

RESULTS

Crystallinity

The crystallinity of each tested material is reported in Table 1. The results indicate that the crystallinity steadily increased as the recycled HDPE content increased. This is because the recycled HDPE used in this study was made from homopolymer with much higher density than the pristine HDPE resin which was a linear copolymer polyethylene used for nonpressure rated pipe.

Incorporating nanoclay also affected the crystallinity of the polymer. Adding 2, 4, and 6 wt% of nanoclay to the recycled blends generally decreased crystallinity. It was reported that the crystalization of polymer can be influenced by the concentration of the nanoclay. At high concentration of nanoclay, silicate layers tend to suppress the crystallization by hindering the mobility of polymer chains and disrupting the crystal growth [4, 23].

Tensile Properties

The tensile properties of tested materials are summarized in Table 1. The data indicate that the yield stress and elastic modulus increased weight content of recycled HDPE. This increase is expected since the tensile properties of semicrystalline polymers are governed by the degree of crystallinity. A higher crystallinity leads to higher tensile properties. However, in the case of nanoclay composites, the mechanical properties increased as the nanoclay content increased even though crystallinity decreased. This is caused by the polymer chains being hindered around the nanoclay platelets which enhances the modulus and yield stress of the composite [24].

DOI 10.1002/pen

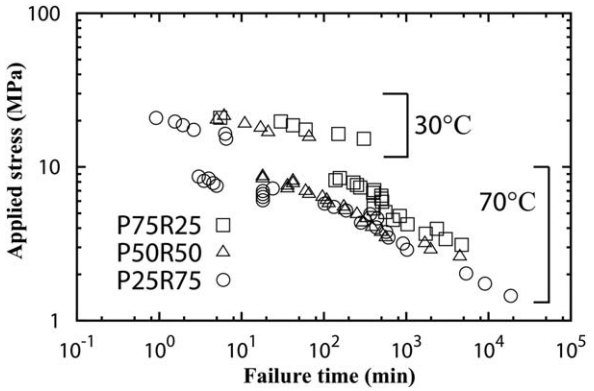

FIG. 1. Data of SCR tests at two testing temperatures.

SCR Test Data

The experimental data from the SCR tests for recycle-blends were presented by plotting the logarithmic applied stress against the logarithmic failure time in Fig. 1. The test data are separated according to the testing temperatures at 30 and 70°C. The SCR test data were extrapolated to generate a single failure curve at 23°C using Popelar's shift method and rate process method in order to correlate with data obtained from the uniaxial tensile test and the essential work of fracture (EWF) test [16, 17].

Popelar's Shift Method (PSM). Popelar et al. [8, 9] developed a bidirectional shifting method based on SCR test data from numerous MDPE and HDPE gas pipe materials at temperatures ranging from 23°C to 96°C. They found that the test data at a specific temperature on log stress-log failure time axes can be bidirectionally correlated with the data at a reference temperature using horizontal and vertical shift factors. The horizontal shifting was achieved by the time-temperature superposition principle while the vertical shifting was related to the effect of temperature on crystallinity of semicrystalline PE.

Rate Process Method. The rate process method (RPM), evolved from the Arrhenius principle of time-temperature superposition, and has been widely used to extrapolate SCR test data to predict the service life of polyethylene materials. The method was standardized in ASTM D2837 [7]. RPM consists of a three-coefficient equation expressing the relationship between stress and failure time with respect to temperature.

Comparing Extrapolated Data from PSM and RPM. A comparison was performed using test data in the brittle failure region of the SCR curves. Samples P25R75 with 2, 4, and 6 wt% of nanoclay were used in the evaluation. For PSM, test data at applied stresses ranging from 1.5 to 3.3 MPa were shifted from the test temperature (70°C) to the reference temperature (23°C). For RPM, an applied stress of 1.7 MPa was tested at 70°C, and 1.5 and 1.7 MPa were used at 80°C. Five replicates were tested at each test condition. Figure 2 presents the predicted curve at 23°C together with the 95% lower confidence interval. Figure 2a and c show that the two extrapolated curves from PSM and RPM for P25R75/2% and P25R75/6% were in good agreement with each other. For P25R75/4% shown in Fig. 2b, PSM slightly under-predicted the failure times in comparison to the mean failure time of RPM. Nonetheless, the extrapolated PSM data of P25R75/4% fell between the 95% confidence interval and mean value of RPM, suggesting that both PSM and RPM produced comparable results for the test materials.

The advantage of applying PSM is that it can directly shift the SCR test data from a single test temperature, while RPM requires multiple testing temperatures to obtain the three coefficients. Since the prediction from the two methods was reasonably similar, PSM was used to predict the failure time at 23°C for all tested materials.

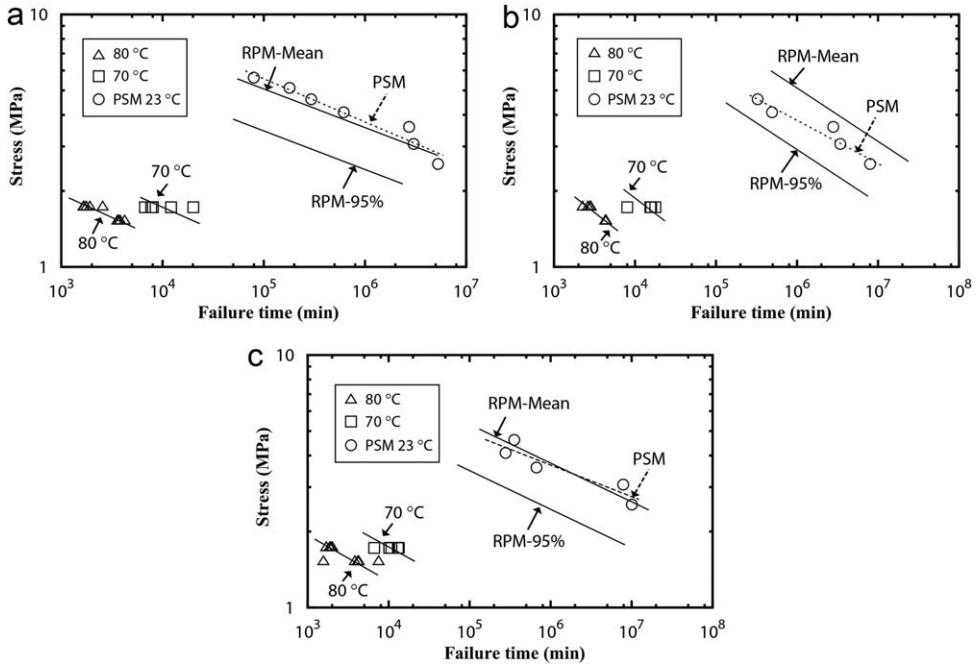

FIG. 2. Comparison of PSM and RPM: (a) P25R75/2%, (b) P25R75/4% and (c) P25R75/6%.

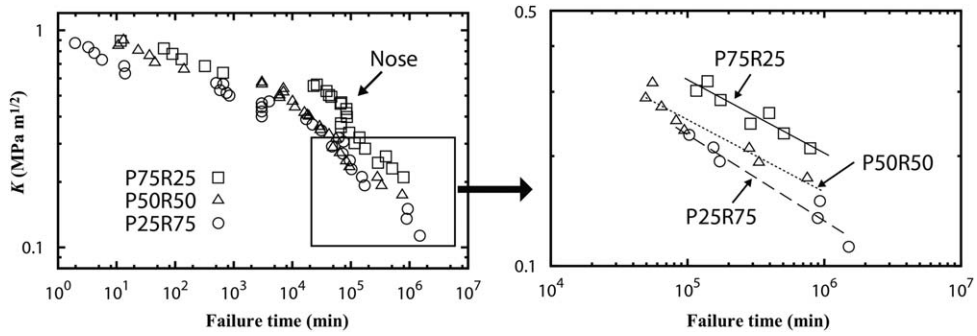

FIG. 3. Log K versus log failure time of recycle-blends: (a) ductile-to-brittle master curve and (b) SCG region.

Linear Elastic Fracture Mechanics (LEFM) Analysis

In analyzing the SCR test data, the load parameter can be expressed by the stress intensity factor K based on LEFM. In mode I fracture, K is expressed as

$$K = F(a/b)\sigma_N\sqrt{\pi a} \tag{1}$$

where $F(a/b)$ [25] is the specimen geometry factor defined by the notch (a)-width (b) ratio, and σ_N is the nominal applied stress.

The SCR test data of recycle-blends at 23°C were predicted using PSM, and the results were presented employing the stress intensity factor K, plotting the log-K against the log-failure time in Fig. 3. The results show a bilinear curve consisting of a shallow linear slope followed by a steeper linear slope. The shallow sloped region corresponded to a ductile failure in which creep is the governing failure mode. In contrast, the steeper sloped region represented a brittle failure mode resulting from a SCG that occurred at lower stresses with longer failure times [26–28].

Increasing the recycled content transformed the transition region of the ductile-to-brittle curve. Hsuan et al. [29] visually categorized the transition types as three different responses: overshoot, trilinear and bilinear. Figure 3a shows that higher content of pristine HDPE (P75R25) exhibited an overshoot type and increased failure times in the transition zone. However, increasing the recycled HDPE content diminished the "Nose" appearance and changed the transition type to bilinear.

Comparing the SCG region of the curves (Fig. 3b), failure times decreased as recycled content increased in the pristine/recycled blends. For example, increasing the recycled content from 25% to 50% decreased the failure time by approximately 70% at the same K condition (0.2 MPa·m$^{1/2}$). Further increase in recycled content to 75% (P25R75) reduced the failure time by 82% compared to the 25% recycled blended material (P75R25). On the other hand, the recycled content had a minimal effect on the slope of SCG.

Figure 4 shows the log-log plots of K versus the failure time of three PCN materials. The nanoclay-reinforced recycle-blends exhibited similar bi-linear failure curve profiles as those from the recycle-blends without nanoclay in Fig. 3a. Thus, the failure mechanism of PCN materials was also dependent on the loading condition (i.e., creep failure at high K whereas SCG failure at low K). Nanoclay from 2 to 6 wt% was incorporated into the P25R75 blend to assess the effect of the nanoclay concentration. Figure 4b shows that the slope of the SCG failure curve decreased as the nanoclay content increased.

EPFM Analysis

In general, LEFM is only applicable for brittle materials that deform linear elastically until fracture occurs or possess a very small region of nonlinear deformation at the crack-tip. However, HDPE is a nonlinear elastic-plastic material; the elastic-plastic fracture parameter (J-integral) should be a more appropriate parameter than K in the evaluation of overall fracture behavior of PE materials [30, 31]. For an elastic-plastic material, the J-integral is determined by a combination of the linear elastic component J^e and the fully plastic component J^p, as expressed in Eq. *2*,

$$J = J^e + J^p \tag{2}$$

The linear elastic component J^e directly relates to the linear elastic stress intensity K while the fully plastic component J^p is dependent on the degree of nonlinearity of a material that can be expressed by the Ramberg-Osgood equation,

$$\frac{\varepsilon}{\varepsilon_0} = \frac{\sigma}{\sigma_0} + \alpha\left(\frac{\sigma}{\sigma_0}\right)^n \tag{3}$$

where σ_0 and ε_0 are typically equal to the yield stress and the corresponding strain, respectively, in the elastic-plastic model. α is a dimensionless constant and n is strain-hardening exponent both of which were obtained by fitting Eq. *3* to the experimental stress-strain tensile test data.

The estimation of the fully plastic component of J (i.e., J^p) with respect to various loading conditions and specimen geometries were given by the Electric Power Research Institute (EPRI) handbook [32]. For the geometry of the single edge notch tension (SENT) specimen, J^p is determined by the following expression,

$$J^p = \alpha\sigma_0\varepsilon_0 c\left(\frac{a}{b}\right)h_{(a/b,\ n)}\left(\frac{P}{P_0}\right)^{n+1} \tag{4}$$

where c denotes the uncracked ligament length. Values of $h_{(a/b,\ n)}$ are provided in the handbook for various a/b and n conditions. All specimens tested in this study have the same notch-width ratio, $a/b = 1/5$. The α and n values can refer to the

 DOI 10.1002/pen

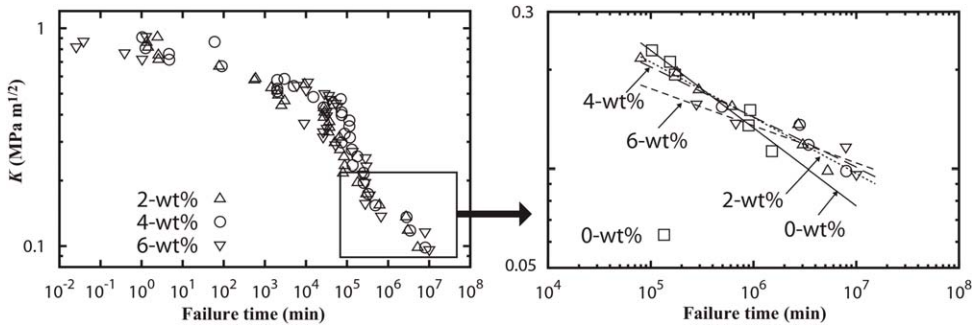

FIG. 4. Log K versus log failure time: (a) P25R75 with 2-, 4- and 6-wt%; (b) SCG region of the curves.

Ramberg-Osgood constants in Eq. *3*. P is the applied load per unit thickness and P_0 is the reference load per unit thickness related to the yield stress, which is given by,

$$P_0 = 1.455\eta c\sigma_0; \text{ plane strain} \tag{5}$$

$$P_0 = 1.071\eta c\sigma_0; \text{ plane stress} \tag{6}$$

where η is defined as

$$\eta = \left[1 + \left(\frac{a}{c}\right)^2\right]^{1/2} - \left(\frac{a}{c}\right) \tag{7}$$

Figure 5 presents the J-integral values calculated from Eqs. *2* through *7* for recycle-blends and PCN materials associated with the failure times for both a plane-strain and plane-stress condition. The discrepancy diminished as the applied stress decreased, showing a convergence of the two curves. At high applied stresses (i.e., high J values) corresponding to short-term failure times, the discrepancy between the two conditions was significant due to the difference of P_0 in J^p (Eqs. *5* and *6*). At high stresses, the crack-tip stress was much greater than the yield stress, leading to a plastic deformation at the region. As a result, the plastic component (J^p) dominated the total J. As the stress decreased, the linear elastic component (J^e) became more dominant in the overall J. Therefore K is not appropriate to expressing the entire stress cracking failure behavior, particularly for the high stress region. On the other hand, at low stress levels where the stress cracking is dominated by the SCG failure, J^e is nearly equal to the total J, indicating that the SCG behavior can be characterized by K.

Correlation between Plane-Strain J and SCG

The failure curve plotting log J versus log failure time in a plan strain condition can be separated into four regions based on the different slopes as illustrated in Fig. 6a. The region I corresponded to the short-term failure where the plastic J (J^p) plays a dominant role in the total J. The applied stresses in this region are higher than the yield stress at 23°C. Once the test specimen being loaded, a small creep zone, which is comparable to a plastic zone, forms instantaneously at the crack-tip (Fig. 6b), and the specimen failed shortly afterward. This implied that the crack growth rate was faster than the growth of the small creep zone. Because the creep zone remained small, it is defined as a small scale creep (SSC) condition and the crack-tip condition can be characterized by J.

In region II, the applied stresses, which are lower than the yield stress at 23°C, enabled the creep zone to grow with time and the creep zone eventually engulfed the entire ligament as illustrated in Fig. 6b. In this condition, both the linear-elastic and the EPFM are unable to characterize the crack-tip condition due to the significant creep strain.

Region III is consistent with the transition from the creep to SCG failure. A large plastic deformation resulting from macroscopic yielding governed the creep failure whereas a craze growing ahead of the crack-tip dominated the SCG failure. These two different mechanisms competed with each other in the transition region [34].

Region IV is dominated by the SCG failure which occurred at much lower applied stresses, typically below 40% of the yield stress. At such low stress, the creep strain is very small. As a result, a SSC condition appeared at the crack-tip and can be characterized by the parameter J [31].

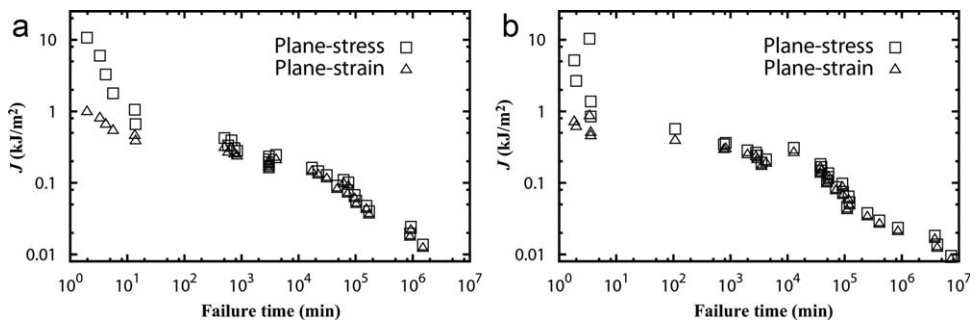

FIG. 5. J-integral versus failure time: (a) P25R75 and (b) P25R75/2%.

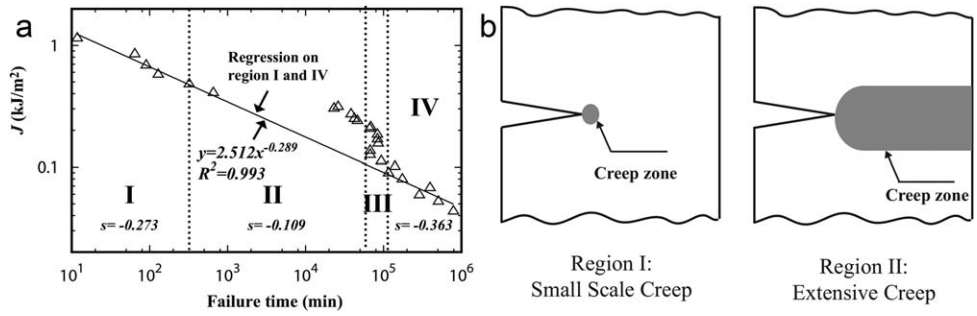

FIG. 6. *J*-failure time plot in the plane-strain condition: (a) experimental data for P75R25 and (b) schematic drawing of creep zone development [33].

Because the fracture behaviors in region I and IV can be characterized by the same parameter J under the assumption of a plane-strain condition, it is reasonable to associate these two regions. Also, the slopes of the test data in the regions I and IV were found to be similar and the data in these two regions can be represented by a single regression line with a very high R^2 value as shown in Fig. 6a. The linear regression line can be expressed as:

$$J = At_f^{-s} \tag{8}$$

where A is the regression constant and s is the slope of the line. t_f denotes the failure time.

Equation *8* implies that the plane-strain fracture toughness (J) can be also calculated once the corresponding failure time is known. In our previous study, the critical J values (J_c) for tested materials were determined using the EWF test together with energy partitioning method [16, 17]. The load-displacement curves obtained from the EWF tests are now converted to load-time curves based on the tensile testing strain rate of 5 mm/min, as illustrated in Fig. 7. The time (t_p) at which the brittle failure occurred is then substituted into Eq. *8* as a t_f value to calculate the corresponding J value, defined as J_{pt} in this article. Table 2 shows the s and t_p value used to calculate the J_{pt}, and the J_c obtained from the EWF test together with the t-statistic value between J_{pt} and J_c.

The similarity of J_c and J_{pt} values for each material was analyzed using t-statistical analysis. When two values are similar, the 95% confidence interval for the difference between them should be less than zero [35]. As shown in Table 2, except for the P25R75/2% sample, the J_{pt} is statistically similar to the J_c. Considering J_c and J_{pt} were obtained from two different test methods, a small discrepancy in one sample should be acceptable. Therefore, the constant A in Eq. *8* could be replaced by the plane-strain fracture toughness J_c once the failure time t_f was normalized by t_p (i.e., unit time $\tau_f = t_f/t_p$), as shown in Eq. *9*.

$$\tau_f = \left(\frac{J}{J_c}\right)^{-1/s} \tag{9}$$

For the recycled blended materials, their slopes (s) are very similar and the J value (J_{pt} or J_c) decreases as the recycled content increases, as shown in Fig. 8a. It can be concluded that failure times in recycle-blends was governed by J_c as illustrated in Fig. 8b. On the other hand, adding nanoclay to recycle-blended materials changed both the slope and J_c. The regression curves shown in Fig. 9 indicate that increasing nanoclay content steadily decreased the slope. Adding nanoclay would lead to a longer failure time, particularly at low J values even though nanoclay caused a decrease in J_c and lowered the failure time at the short-term failure region.

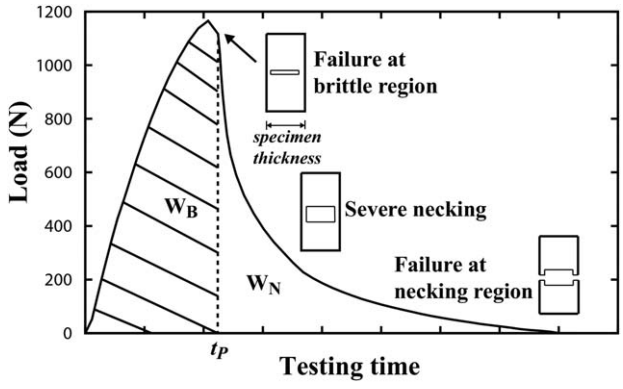

FIG. 7. Energy partitioning method (W_B: fracture energy within brittle failure and W_N: fracture energy within necking region).

DISCUSSION

In this article, the short-term fracture toughness parameter J_c is experimentally correlated with the long-term SCG behavior based on the conventional EPFM. A similar approach which correlated J_c with the SCG data was reported by Zhou et al. [14]. They determined the relationship between the time to failure t_f and J of SCG employing LEFM under a plane-strain condition (i.e., $J = J^e$). However, they did not consider the short-term failure region in which J^p became the governing parameter. This study accounted

TABLE 2. Comparison between the specific EWF (J_c) and J_{pt} values for recycle blends and PCNs.

Sample	s	R^2	t_p (min)	J_{pt} (kJ/m^2)	J_c (kJ/m^2)	t-statistic
P75R25	0.289	0.99	0.19	3.35–4.99	2.47–8.97	−2.007
P75R25/2%	0.275	0.98	0.13	2.74–6.04	4.73–6.77	−0.993
P50R50	0.310	0.99	0.13	3.14–4.58	2.67–5.29	−1.810
P50R50/2%	0.291	0.99	0.10	2.33–3.41	2.74–4.38	−0.536
P25R75	0.303	0.98	0.12	1.52–2.78	1.48–4.20	−0.839
P25R75/2%	0.276	0.99	0.09	1.11–2.01	2.03–3.73	0.169
P25R75/4%	0.272	0.99	0.07	1.07–1.85	0.31–2.59	−1.306
P25R75/6%	0.233	0.97	0.08	0.42–1.16	0.50–2.14	−0.485

DOI 10.1002/pen

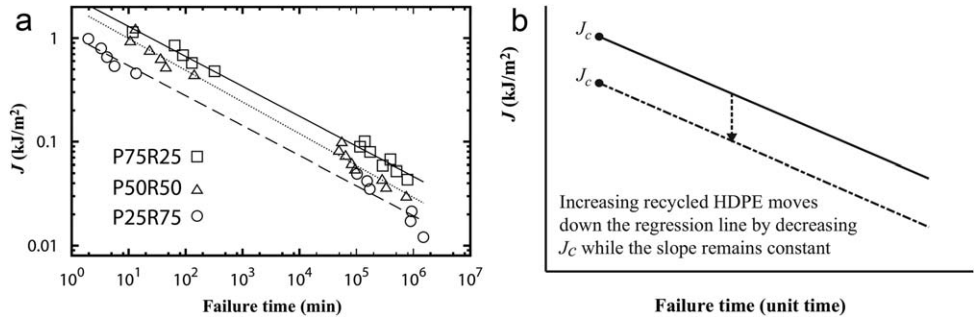

FIG. 8. (a) Effect of recycled HDPE content on *J*-failure time response and (b) schematic drawing of the effect.

for the highly nonlinear elastic-plastic fracture in the short-term failure region based on EPFM, and therefore, provided a comprehensive relationship between J_c and SCG.

The *J*-integral analysis revealed that the failure time in association with the SCG mechanism of recycle-blends was governed by J_c. An increase in recycled HDPE content lowered J_c, resulting in shortening the failure time of SCG while the slope is independent of the recycled content (Fig. 8a and b). Adding and increasing the nanoclay content reduced J_c and subsequently decreased the failure times at high *J* values (i.e., the short-term failure region); however, it also decreased the slope (i.e., rate of SCG), and thus the failure times at low *J* values increased (Fig. 9b).

Understanding the mechanism that causes the change in the slope would gain insight into the effect of nanoclay on stress cracking behavior. Williams and Marshall [15] proposed a relaxation-controlled growth theory that correlates the fracture initiation time (t_B) in SCG and the corresponding stress intensity factor *K* in polymers. They found that t_B is related to the time-dependent response of the craze zone stress and modulus as expressed in Eq. *11* if the time dependence of the relaxation stress and modulus can be represented by a power law.

$$t_B \sim K^{-2/(m+n)} \tag{11}$$

The exponent parameters *m* and *n* are the time-dependent response of the stress and modulus to produce the craze.

Both Eqs. 10 and *11* express the relationship between time and fracture parameter in a similar form. Thus, it can be assumed that the slope in Eq. 10 is also related with the time-dependent response of a material. Zhong et al. [36] and Wang et al. [37] reported that the stress relaxation of a PCN system is dependent on the nanoclay-polymer interaction. The nanoclay confines the mobility of adjacent polymer molecular chains and hinders the relaxation of polymer. Therefore, PCN requires a longer relaxation time than unreinforced polymer at a given stress. An increase in the relaxation time by nanoclay reflects a decrease of *m* and *n* (i.e., decrease of the slope in Fig. 9), resulting in the extended failure time in SCG.

CONCLUSIONS

The effect of nanoclay on the long-term stress cracking behavior of recycled HDPE blends was studied. The stress cracking property was evaluated using the NCLS test, and the test data were subsequently analyzed using the stress intensity factor *K* and the *J*-integral. Applying the *J*-integral approach, a correlation integrating J_c and SCG was established under the assumption of a plane-strain condition. Furthermore, the results indicated that replacing pristine HDPE with recycled bottle grade HDPE reduced the short-term fracture toughness J_c and thus decreased failure times of SCG; the failure time reduction increased with the recycled weight content. On the other hand, incorporating nanoclay up to 6 wt% lowered the J_c value as well as the slope of the SCG failure curves, subsequently increasing the failure time in the lower *J* values. Therefore, nanoclay can be used as an additive to enhance the SCG resistance of pristine HDPE and recycled HDPE blended materials for pipe and other products.

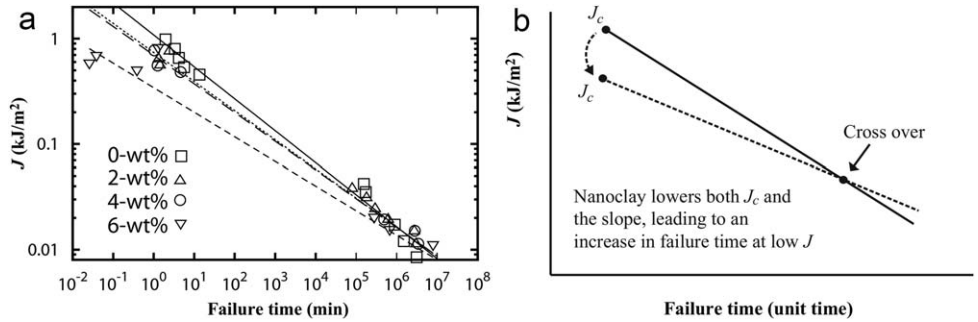

FIG. 9. Effect of nanoclay content on *J*-failure time behavior: (a) P25R75 with 2-, 4-, and 6-wt% nanoclay and (b) schematic drawing of the effect.

ACKNOWLEDGMENT

Any opinions, findings, and conclusions or recommendations expressed in this material are those of the authors and do not necessarily reflect the views of the National Science Foundation.

REFERENCES

1. L. Nguyen, G.Y. Hsuan, and S. Spatari, *J. Polym. Environ*., (2016). [TQ1]
2. V. Stefanovski, S. Masood, E. Koslor, P. Iovenitti, and I. Sbarski, *Pipes from Recycled High Density Polyethylene Blends*. ANTEC, SPE (2002).
3. Y. Hsuan, *PPI report published by Plastic Pipe Institute*, Washington, DC (1997).
4. A. Mudaliar, Q. Yuan, and R. Misra, *Polym. Eng. Sci*., **46**, 1625 (2006).
5. J.W. Gilman, C.L. Jackson, A.B. Morgan, R. Harris, E. Manias, E.P. Giannelis, M. Wuthenow, D. Hilton, and S.H. Phillips, *Chem. Mater*., **12**, 1866 (2000).
6. Q.H. Zeng, A.B. Yu, G.Q. Lu, and D.R. Paul, *J. Nanosci. Nanotechnol*., **5**, 1574 (2005).
7. ASTM D2837. Obtaining Hydrostatic Design Basis for Thermoplastic Pipe Materials or Pressure Design Basis for Thermoplastic Pipe Products. West Conshohocken, PA: ASTM International, 2013.
8. C.F. Popelar, C.H. Popelar, and V.H. Kenner, *Polym. Eng. Sci*., **30**, 577 (1990).
9. C.H. Popelar, V.H. Kenner, and J.P. Wooster, *Polym. Eng. Sci*., **31**, 1693 (1991).
10. M. McCarthy, R. Deblieck, P. Mindermann, R. Kloth, L. Kurelec, and H. Martens, *Budapest*, (2008).
11. ISO 18488. Determination of Strain Hardening Modulus in relation to slow crack growth Geneva, Switzerland: International Organization for Standardization, 2015.
12. P.W.R. Beaumont, and R.J. Young, *J. Mater. Sci*., **10**, 1334 (1975).
13. R.J. Young, and P.W.R. Beaumont, *Polymer*, **17**, 717 (1976).
14. Z. Zhou, N. Brown, and B. Crist, *J. Polym. Sci. B Polym. Phys*., **33**, 1047 (1995).
15. J.G. Williams, and G.P. Marshall, *Environmental Crack and Craze Growth Phenomena in Polymers*, Proceedings of the Royal Society A, **25**, (1975).
16. S. Na, S. Spatari, and Y.G. Hsuan, *Eng. Fract. Mech*., **139**, 1 (2015).
17. S. Na, S. Spatari, and Y.G. Hsuan, *Polym. Eng. Sci*., **56**, 222 (2016).
18. S. Na, L. Nguyen, S. Spatari, and G.Y. Hsuan, Evaluating the Effect of Nanoclay and Recycled HDPE on Stress Cracking in HDPE using J-Integral Approach. ANTEC. Indianapolis, IN, 2016.
19. ASTM D4703. Standard Practice for Compression Molding Thermoplastic Materials into Test Specimens, Plaque, or Sheets. West Conshohocken, PA: ASTM International, 2010.
20. ASTM D3418. Transition Temperatures and Enthalpies of Fusion and Crystallization of Polymers by Differential Scanning Calorimetry. West Conshohocken: ASTM International 2003.
21. ASTM D638. Tensile Properties of Plastics. West Conshohocken, PA: ASTM International, 2003.
22. ASTM F2136. Notched, Constant Ligament-Stress (NCLS) Test to Determine Slow-Crack-Growth Resistance of HDPE Resins or HDPE Corrugated PIPE. West Conshohocken, PA: ASTM International, 2008.
23. T.D. Fornes, and D.R. Paul, *Polymer*, **44**, 3945 (2003).
24. Y. Kojima, A. Usuki, M. Kawasumi, A. Okada, Y. Fukushima, T. Kurauchi, and O. Kamigaito, *J. Mater. Res*., **8**, 1185 (1993).
25. H. Tada, P.C. Paris, and G.R. Irwin, *The Stress Analysis of Cracks Handbook*, ASME Press, New York, 2000.
26. N. Brown, and X. Lu, *Polymer*, **36**, 543 (1995).
27. X. Lu, and N. Brown, *J. Mater. Sci*., **25**, 29 (1990).
28. Y. Grace Hsuan, *Geotextiles Geomembr*., **18**, 1 (2000).
29. Y. Hsuan, R. Koerner, and A. Lord, *Geotech. Test. J*., **16**, (1993).
30. J.L. Bassani, N. Brown, and X. Lu, *Int. J. Fract*., **38**, 43 (1988).
31. X. Lu, N. Brown, and J.L. Bassani, *Polymer*, **30**, 2215 (1989).
32. V. Kumar, M. D. German, and C. F. Shih, An Engineering Approach for Elastic-Plastic Fracture Analysis. Palo Alto, CA, USA: EPRI, 1981.
33. A. Saxena, *Nonlinear Fracture Mechanics for Engineers*, CRC Press, Chicago (1998).
34. N. Brown, J. Donofrio, and X. Lu, *Polymer*, **28**, 1326 (1987).
35. A. Knezevic, Overlapping confidence intervals and statistical significance. StatNews: Cornell University Statistical Consulting Unit 73, 1 (2008).
36. Y. Zhong, Z. Zhu, and S.-Q. Wang, *Polymer*, **46**, 3006 (2005).
37. K. Wang, S. Liang, J. Deng, H. Yang, Q. Zhang, Q. Fu, X. Dong, D. Wang, and C.C. Han, *Polymer*, **47**, 7131 (2006).

 DOI 10.1002/pen